

Testing white dwarf cosmochronology using wide double white dwarfs

Tyler Heintz¹ and JJ Hermes

Institute for Astrophysical Research, Boston University, 725 Commonwealth Ave,
Boston MA 02215, USA

Abstract. We present a sample of nearly 650 widely separated double white dwarf binaries found using Gaia DR2 astrometry. We derive preliminary total ages for each white dwarf in our sample using Gaia photometry and compare the total ages of both components of each binary in our sample. We find agreement within 3 sigma between the two ages $\sim 85\%$ of the time with median age uncertainties of ~ 3.5 Gyr depending on which initial-final mass relation is used. When a subsample with the most precise ages is used, the agreement within 3 sigma drops to $\sim 70\%$ with median age uncertainties of 300-600 Myr.

Keywords. white dwarfs, binary stars, ages

1. Introduction

In the age of Gaia, searches for widely separated (>100 AU) binary systems are uncovering large numbers of systems (e.g. $>50,000$ from [El-Badry & Rix 2018](#)). These systems provide great test beds for multiple areas of galactic and stellar astrophysics. For example, they have been used to study the galactic gravitational potential (i.e. [Correa-Otto et al. 2017](#)). In addition, wide binaries provide two coeval objects that can be used to test and calibrate current ageing techniques.

White dwarfs have been used as cosmochrometers for more than 30 years (See review by [Fontaine et al. 2001](#)). White dwarfs have been used to age a variety of astronomical objects including binary companions (i.e. [Fouesneau et al. 2019](#)) and the halo and disk of our own galaxy (i.e. [Winget et al. 1987](#); [Kilic et al. 2019](#)). Due to its relatively simple and characteristic cooling, the mass and effective temperature of a white dwarf can be uniquely mapped to a cooling age. To determine the total age of a white dwarf from the main sequence to its current state, a relation between its current mass as a white dwarf and its zero-age main sequence mass is needed. This can be done using an empirical, cluster calibrated initial-final mass relation (i.e. [Catalán et al. 2008](#); [Salaris et al. 2009](#); [Cummins et al. 2018](#)). This method gives a model-dependent total age of the white dwarf.

In this paper, we present a sample of 642 wide white dwarf white dwarf binaries and a comparison of total ages of the two components of each binary. In Section 2, the method of finding these binaries is discussed along with the ageing technique used. In Section 3, we present a preliminary attempt to compare total ages in these wide binaries. We end with a discussion of our results and future work in Section 4.

2. Methods

2.1. Generation of Binary Catalog

To generate the wide double white dwarf sample, we take a similar approach to [El-Badry & Rix \(2018\)](#). For a full discussion of the binary search along with the relevant quality cuts and binary pair criteria, see [El-Badry & Rix \(2018\)](#).

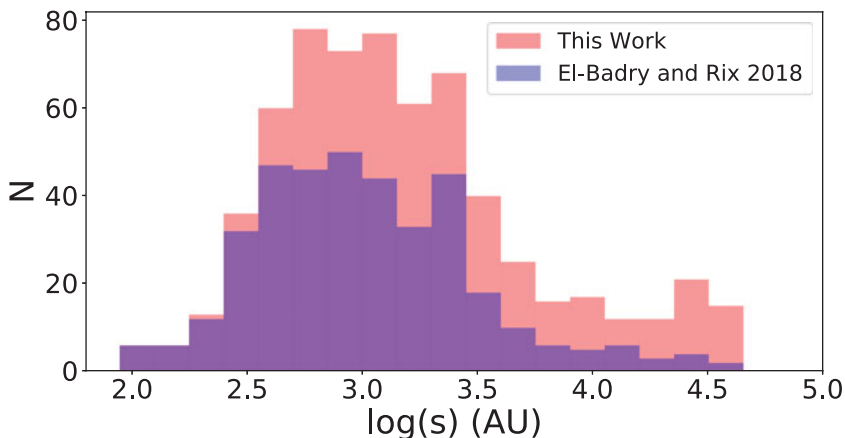


Figure 1. The separation distribution of our 642 wide WD/WD binaries in red with the wide WD/WD binaries from [El-Badry & Rix \(2018\)](#) in blue.

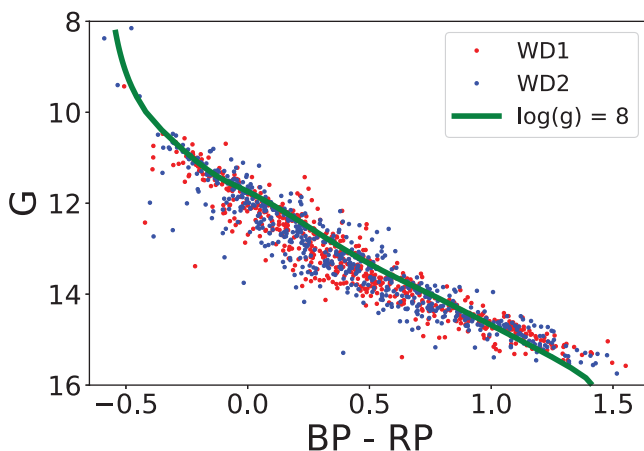


Figure 2. An H-R diagram of 580 of our 642 binaries where both white dwarfs have a probability of being a white dwarf higher than 0.8 from [Gentile Fusillo *et al.* \(2019\)](#). A curve for $\log(g) = 8$ white dwarfs is provided in green as well taken from [Tremblay *et al.* \(2009\)](#).

We make a few changes to their search that favor white dwarfs and are aimed to generate the largest sample possible. They use the full Gaia catalog, a strict 200 parsec cutoff, and an upper bound orbit velocity with a total mass of 5 solar masses. In contrast, we use the Gaia DR2 white dwarf catalog from [Gentile Fusillo *et al.* \(2019\)](#), no distance cutoff, and an upper bound orbit velocity with a total mass of 2.8 solar masses.

With these changes, we increase the sample of 375 wide WD/WD binaries from [El-Badry & Rix \(2018\)](#) to 642. The separation distribution and an H-R diagram of our sample can be seen in Figures 1 and 2 respectively. We find more binaries at all separations and recover all but two of the 375 binaries from [El-Badry & Rix \(2018\)](#).

2.2. White Dwarf Ageing

To determine the total age of a white dwarf, a cooling age and main sequence lifetime is needed. To calculate the cooling ages of our white dwarfs, effective temperatures and masses are needed. As a preliminary age determination, we only use the photometrically

determined effective temperatures and masses from the Gaia DR2 white dwarf catalog [Gentile Fusillo *et al.* \(2019\)](#). To get the cooling ages from these masses and effective temperatures, we use the Montréal white dwarf cooling models [Tremblay *et al.* \(2009\)](#); [Bergeron *et al.* \(2011\)](#). These cooling models need to know the spectral type of the white dwarf. Different atmospheric compositions have varying effects on the cooling rates of these stars. When a spectral type is available, we use the corresponding model. If no spectral type is known, then a DA white dwarf is assumed.

A progenitor main sequence mass must be found to determine the main sequence lifetimes of each of our white dwarfs. The main sequence masses are determined through the use of an empirical initial-final mass relation. We use three separate initial final mass relations to get a better understanding of the empirical uncertainty in the main sequence lifetimes. The three that are used are from [Cummings *et al.* \(2018\)](#), [Salaris *et al.* \(2009\)](#), and [Catalán *et al.* \(2008\)](#). Once the progenitor main sequence masses are determined, MESA stellar evolutionary tracks ([Dotter 2016](#); [Choi *et al.* 2016](#); [Paxton *et al.* 2011, 2013, 2015](#)) are used to derive the main sequence lifetimes.

To determine the uncertainties on the total ages, we take a simple approach. We use the one sigma error bars on the mass and effective temperatures to derive total ages with the upper and lower masses and effective temperatures. This gives us a range on the total age. We leave more rigorous error analysis to future work.

3. Age Comparison

The two stars in a binary system are formed at nearly the same time from the same collapsing cloud of gas. Thus, the two white dwarfs in each of the wide binaries from our sample should have the same total age.

Using the ageing methods discussed in Section 2.2, we find that the total ages of the two component white dwarfs of each binary agree within 3 sigma 90%, 80%, and 89% of the time for the initial-final mass relations from [Cummings *et al.* \(2018\)](#), [Salaris *et al.* \(2009\)](#), and [Catalán *et al.* \(2008\)](#), respectively. The median uncertainties from each were 3.8, 0.75, and 3.7 Gyr, respectively. This only includes 200-300 systems depending on the lower and upper cutoffs for each initial-final mass relation used. If a system has one of its components that is below or above these bounds, its ages cannot be compared. A histogram of the number of standard deviations away from zero age difference for these systems can be seen in Figure 3.

Since these median errors are so large, we construct a subsample where one of the two components of the binary has an age uncertainty less than 1 Gyr. In this subsample, we find agreement within 3 sigma 77%, 63%, and 66% of the time. The median uncertainties for this subsample are 0.625, 0.335, and 0.425 Gyr. These subsamples contain around 65-75 systems that can have the ages compared due to the bounds on the initial-final mass relations. A histogram of the number of standard deviations away from zero age difference for these systems can be seen in Figure 3.

4. Summary and Future Work

We have developed the largest wide double white dwarf catalog to date using Gaia DR2. Using similar methods to [El-Badry & Rix \(2018\)](#), we find 642 wide double white dwarf binaries that span most of the typical region where white dwarfs are found in the Gaia color-magnitude diagram. We make changes to their search to be tailored for finding specifically double white dwarfs. We use a total mass of 2.8 solar masses for the maximum bound orbital velocity instead of 5 solar masses, and we make no strict distance cutoff. In the future, less strict photometric cuts can be made to add additional to white dwarfs.

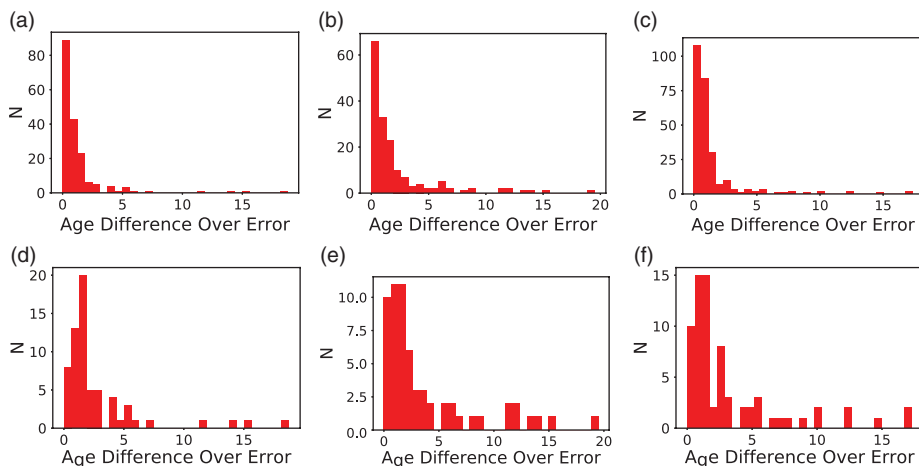


Figure 3. The top three panels show the age difference over error for the two components in each wide double white dwarf binary in our sample using the (a) Cummings *et al.* (2018), (b) Salaris *et al.* (2009), and (c) Catalán *et al.* (2008) initial-final mass relations. The histograms show 180, 168, 263 systems respectively due to the different bounds on the initial-final mass relation. The bottom three panels show the age difference over error for the two components in each wide double white dwarf binary in our subsample with more precise ages using the (d) Cummings *et al.* (2018), (e) Salaris *et al.* (2009), and (f) Catalán *et al.* (2008) initial-final mass relations. The histograms show 65, 61, 71 systems respectively due to the different bounds on the initial-final mass relation.

Since binary star systems form at approximately the same time, both white dwarfs in these systems should have the same age. We performed a preliminary check to see if our systems exhibit this age agreement by using the white dwarf ageing techniques discussed in Section 2.2. We find that the ages agree within 3 sigma 90%, 80%, and 89% of the time for the initial-final mass relations from Cummings *et al.* (2018), Salaris *et al.* (2009), and Catalán *et al.* (2008), respectively. When limiting to the systems with one white dwarf with less than a Gyr uncertainty, the 3 sigma agreement drops to 75%, 65%, and 70%, respectively. These ages are very preliminary and only provide a brief check for “ill-behaved” systems. These ill-behaved systems could provide insights into previous merger history or may provide insights into the nature of the true initial-final mass relation. Future work will be focused on studying these ill-behaved systems with follow-up observations. Additionally, future work will aim to add more photometric bandpasses to develop a broadband SED to get improved photometric surface gravities and effective temperatures which will provide more reliable and precise ages.

Acknowledgements

We thank Kareem El-Badry for helpful discussions. This work was partially supported by the Massachusetts Space Grant Consortium.

References

- Bergeron, P., Wesemael, F., Dufour, P., *et al.* 2011, *ApJ*, 737, 28
 Catalán, S., Isern, J., García-Berro, E., & Ribas, I. 2008, *MNRAS*, 387, 1693
 Choi, J., Dotter, A., Conroy, C., *et al.* 2016, *ApJ*, 823, 102
 Correa-Otto, J. A., Calandra, M. F., & Gil-Hutton, R. A. 2017, *A&A*, 600, A59
 Cummings, J. D., Kalirai, J. S., Tremblay, P. E., Ramirez-Ruiz, E., & Choi, J. 2018, *ApJ*, 866, 21
 Dotter, A. 2016, *ApJS*, 222, 8
 El-Badry, K. & Rix, H.-W. 2018, *MNRAS*, 480, 4884

- Fontaine, G., Brassard, P., & Bergeron, P. 2001, *PASP*, 113, 409
- Fouesneau, M., Rix, H.-W., von Hippel, T., Hogg, D. W., & Tian, H. 2019, *ApJ*, 866, 21
- Gentile Fusillo, N. P., Tremblay, P.-E., Gänsicke, B. T., *et al.* 2019, *MNRAS*, 482, 4570
- Kilic, M., Bergeron, P., Dame, K., *et al.* 2019, *MNRAS*, 482, 965
- Paxton, B., Bildsten, L., Dotter, A., *et al.* 2011, *ApJS*, 192, 3
- Paxton, B., Cantiello, M., Arras, P. *et al.* 2013, *ApJS*, 208, 4
- Paxton, B., Marchant, P., Schwab, J. *et al.* 2015, *ApJS*, 220, 15
- Salaris, M., Serenelli, A., Weiss, A., & Miller Bertolami, M. 2009, *ApJ*, 692, 1013
- Tremblay, P. E., Bergeron, P., & Gianninas, A. 2011, *ApJ*, 730, 128
- Winget, D. E., Hansen, C. J., Liebert, J., *et al.* 1987, *ApJ*, 315, L77